ISSN 0965-545X, Polymer Science, Series A, 2021, Vol. 63, No. 3, pp. 296–306. © The Author(s), 2021. This article is an open access publication, corrected publication 2021.
Russian Text © The Author(s), 2021, published in Vysokomolekulyarnye Soedineniya, Seriya A, 2021, Vol. 63, No. 3, pp. 198–209.

COMPOSITES

Magnetorheological Fluids Based on Star-Shaped and Linear Polydimethylsiloxanes

S. A. Kostrov[a,b], P. A. Tikhonov[c], A. M. Muzafarov[a,b,c], and E. Yu. Kramarenko[a,b,*]

[a] *Faculty of Physics, Moscow State University, Moscow, 119991 Russia*
[b] *Nesmeyanov Institute of Organoelement Compounds, Russian Academy of Sciences, Moscow, 119991 Russia*
[c] *Enikolopov Institute of Synthetic Polymer Materials, Russian Academy of Sciences, Moscow, 117393 Russia*
**e-mail: kram@polly.phys.msu.ru*

Received November 26, 2020; revised December 25, 2020; accepted January 11, 2021

Abstract—Magnetorheological fluids are obtained on the basis of star-shaped and linear PDMS containing 70, 75, and 80 wt % of carbonyl iron microparticles. While pure PDMS polymers are Newtonian fluids, composites exhibit pseudoplasticity. The viscoelastic properties of the obtained magnetorheological fluids of different composition are studied in magnetic fields up to 1 T. The viscosity and storage modulus of the magnetorheological fluids in the maximum magnetic field reach ~0.19–0.65 MPa s and 0.4 MPa, respectively. The relative increase in the viscosity and storage modulus of the magnetorheological fluids based on the star-shaped PDMS with a magnetic filler concentration of 70 wt % in a magnetic field exceeds four orders of magnitude. In the magnetic field, the yield stress of the magnetic composites is as high as 70 kPa at a magnetic field strength of 1 T.

DOI: 10.1134/S0965545X2103007X

INTRODUCTION

Magnetorheological fluids (**MRFs**) are composite materials consisting of magnetic microparticles placed in a liquid nonmagnetic medium [1, 2]. MRFs belong to the class of the so-called smart materials, the physical properties of which can change with changing external conditions. Under application of an external magnetic field, magnetic filler particles are arranged in chain aggregates directed along the magnetic field lines. The rearrangement of the internal structure of the composite leads to significant changes in such characteristics of the material as the electrical and thermal conductivity, dielectric constant, viscosity, and elastic modulus; the changes can reach several orders of magnitude [3–6]. The unique properties of MRFs and the ability to control them by means of external magnetic fields open up broad prospects for their practical application. The typical examples of devices based on MRFs are dampers [7–13], brakes [14–16] and clamping mechanisms [17–19].

Depending on the task, various liquids can be used as a dispersion medium: water [20–22], polyesters [23], synthetic hydrocarbons, and mineral or silicone oils [24]. In particular, MRFs based on mineral oils and organosilicon compounds are employed in lubrication and sealing systems and water-based MRFs are used in medicine.

In this work, the possibility of using polydimethylsiloxane oligomers as a dispersion medium is studied. It is known that PDMS is a bioinert material which makes it possible to potentially use PDMS-based MRFs in medicine. The polymer medium has a specific rheology: it can exhibit non-Newtonian behavior and has a higher viscosity than low molecular weight liquids. Therefore, the use of oligomers instead of a low molecular weight liquid improves the sedimentation stability of MRFs. However, it should be noted that a medium with a viscosity of ~1 Pa s still cannot provide good stability of devices on time scales much longer than 24 h. An additional increase in the sedimentation stability of the composite can be achieved with the use of special additives [25, 26] or by chemical grafting of polymer onto the surface of magnetic particles [26–28].

The paper compares the viscoelastic properties of MRFs based on the linear and 32-arm star-shaped PDMS. Earlier, MRFs based on hyperbranched macromolecules were studied [29]. At the same molecular weight, star-shaped macromolecules have a lower viscosity than linear ones. Therefore, it can be expected that MRFs based on a star-shaped polymer will exhibit a greater magnetic response, since the restructuring of magnetic filler particles in a less viscous medium occurs more easily and hysteresis phenomena are less pronounced. In addition, the use of star-shaped molecules as dispersion media opens up new possibilities for controlling the properties of MRFs. In particular, the introduction of functional groups at the ends of the

arms can lead to an increase in the compatibility of the matrix with magnetic particles or to additional structuring of the medium due to the aggregation of functional groups. This can be useful for both MRFs and crosslinked magnetic composites.

The aim of this work is a comprehensive comparative analysis of the viscoelastic properties of MRFs based on linear and star-shaped PDMS with different contents of the magnetic filler in external magnetic fields up to 1 T.

MATERIALS

Carbonyl iron (P20 grade, Vekton) with an average particle size of 4.5 μm was used as a magnetic filler.

Linear PDMS with an average molecular weight of $M_n = 3.6 \times 10^4$, $Đ = 1.67$ was derived from α,ω-divinyldimethylsiloxane (Vinyl Silicone Oil 5000 cSt grade, Penta-91).

A 32-arm star-shaped PDMS was synthesized according to the method described in detail in [30, 31] and in the file with supplementary materials. The following materials were used for its synthesis: 1,1,3,3,5,5-hexamethylcyclotrisiloxane (**D_3**) (95%, ABCR) dried and distilled over calcium hydride, *n*-butyllithium as a 1.6 M solution in hexane (Acros), the initial carbosilane dendrimer of the fourth generation with DDMS protecting groups synthesized at the Enikolopov Institute of Synthetic Polymeric Materials of the Russian Academy of Sciences according to the method described in [30, 31], tetramethylethylenediamine (99%, Acros) dried over 3 Å molecular sieves, petroleum ether distilled on a rotary evaporator (OOO Ruskhim.ru), silica gel (Merk Kiesegel 60, 0.040–0.063 mm, pH 6.5–7.5), anhydrous sodium sulfate (OOO Komponent-reaktiv), hexane (97.76%, OOO Ruskhim.ru) dried over calcium hydride and 3 Å molecular sieves, toluene of analytical grade (OOO Khimpromtorg) dried over sodium with benzophenone and 3 Å molecular sieves, and tetrahydrofuran (99.8%, OOO Ruskhim.ru) dried over sodium with benzophenone and 3 Å molecular sieves.

The molecular weight of the resulting star-shaped PDMS (NMR data) was $M_n = 12.9 \times 10^4$, $Đ = 1.11$, and the average arm length was 46 dimethylsiloxane units.

RESEARCH METHODS

The viscoelastic properties of the star-shaped and linear PDMS and their magnetic composites were studied on an Anton Paar Physica MCR 302 rheometer with a plate–plate measuring system and an MRD 170/1 T magnetic cell equipped with an electromagnet. A layer of magnetic fluid with a height of h = 0.1 mm was applied between the measuring head connected to the rotor and the surface of the fixed substrate (Fig. 1). The viscosity of liquids η was measured in a rotation mode in the range of shear rates $\dot{\gamma} = 0.01–100$ s^{-1}. Dynamic measurements were also carried out in the mode of forced torsional oscillations, in which the shear strain of the samples was varied according to the harmonic law $\gamma = \gamma_0 \sin(\omega t)$, where γ is strain, γ_0 is the strain amplitude, and ω is the frequency of shear oscillations. The shear elastic modulus (the storage modulus) G', which is responsible for the elastic response of the material, and the shear loss modulus G'', which characterizes the viscous response associated with energy dissipation in the sample, were assessed. The frequency dependences were measured at a fixed oscillation amplitude $\gamma_0 = 0.1\%$ in the frequency range $\omega = 1–100$ rad/s, and the amplitude dependences were measured at a fixed oscillation frequency $\omega = 10$ rad/s in the range of oscillation amplitudes $\gamma_0 = 0.02–20\%$. The magnetic field set by an electromagnetic field and directed perpendicular to the shear plane was varied up to $B = 1$ T.

Before each measurement, the liquid was rotated at a shear rate of $\dot{\gamma} = 100$ s^{-1} for 60 s. After each measurement in the magnetic field, the liquid was renewed. These two conditions made it possible to provide the same initial conditions for subsequent measurements. The same method was used, for example, in [32].

The GPC analysis of the star-shaped PDMS was carried out on a chromatographic system including a STAYER s. 2 high-pressure pump (Akvilon, Russia), a Smartline RI 2300 refractometer, and a JETSTREAM 2 PLUS thermostat (Knauer, Germany). Analysis conditions: the thermostat temperature, 40°C (±0.1°C); eluents, THF and toluene + 2% THF; the flow rate, 1.0 mL/min; columns, 300 × 7.8 mm; 5 μm Phenogel sorbent (Phenomenex, United States); pore size, 10^3 Å.

^{1}H NMR spectra were measured on a Bruker Avance AV300 spectrometer (solvent, $CDCl_3$; ACD LABS program; external standard, tetramethylsilane; solvents, *n*-hexane and $CDCl_3$).

Analysis results for intermediate and final products are available in Supplementary Materials.

RESULTS AND DISCUSSION

Rheological Properties of Unfilled Fluids

The flow curves of the star-shaped and linear PDMS were measured at different temperatures (Fig. 2). In the investigated temperature range, both liquids exhibit behavior close to Newtonian. The same result for 32-arm stars was reported in [33]. A slight deviation from the Newtonian behavior is observed at elevated temperatures, but viscosity changes do not exceed 20% with an increase in the shear rate by three orders of magnitude. It can be expected that physical entanglements do not make a significant contribution to the rheological properties of both star-shaped and linear PDMS owing to their low molecular weight (the molecular weight of linear PDMS is close to the criti-

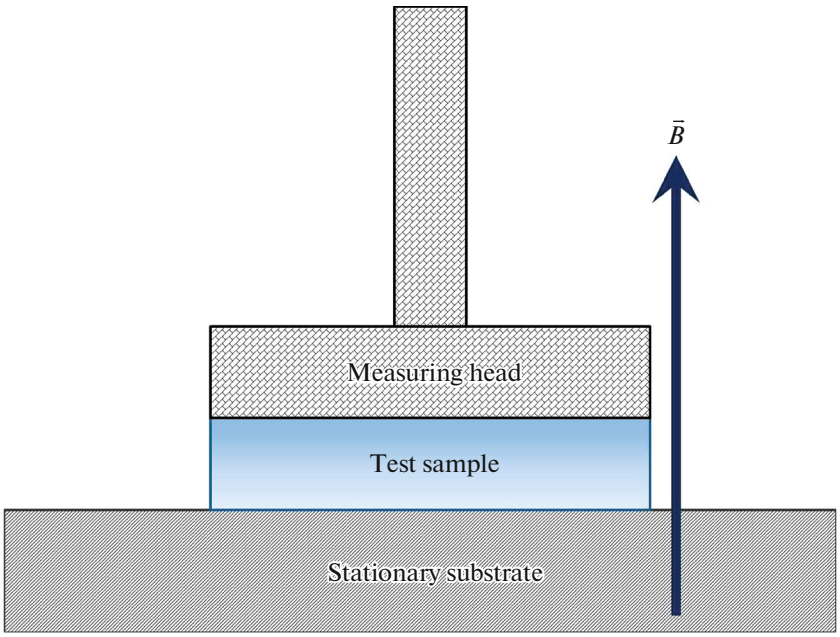

Fig. 1. Measuring unit diagram for rheological measurements. Color drawings can be viewed in the electronic version.

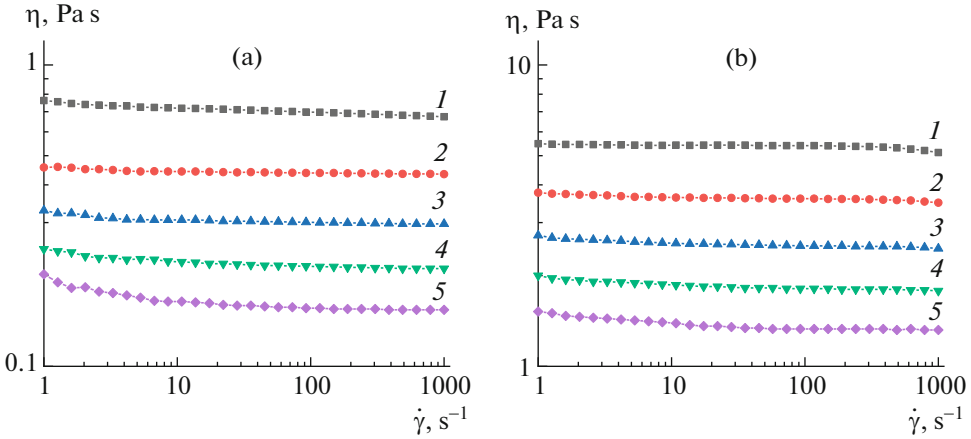

Fig. 2. Dependences of the viscosity of (a) star-shaped and (b) linear PDMS on the shear rate at (*1*) 20, (*2*) 40, (*3*) 60, (*4*) 80, and (*5*) 100°C.

cal value $M_{cr} \sim 3.0 \times 10^4$, at which entanglements begin to form in the melt [34, 35]). The viscosity values obtained at room temperature are 0.8 Pa s for the star-shaped PDMS and 5.5 Pa s for the linear PDMS. The viscosity of linear PDMS is significantly higher than that of the star-shaped counterpart despite its lower molecular weight. This result may be explained by the fact that a star-shaped molecule has a more compact structure due to the presence of branching points, and the span of the star-shaped PDMS is ~5 times less than the chain length of a linear molecule. In this case, the activation energies of the viscous flow E_a calculated from the temperature dependences of viscosity according to the Arrhenius equation (Fig. 3) are almost the same and amount to 17.0 kJ/mol for the star-shaped PDMS and 15.5 kJ/mol for the linear PDMS. The branched structure of the star-shaped polymer does not significantly affect the value of E_a.

Magnetorheological Properties of MRFs

Magnetorheological fluids were prepared by the mechanical mixing of the corresponding polymer and carbonyl iron (particle size, 3–5 μm). The content of the magnetic filler in MRF-70, MRF-75, and MRF-80 samples was 70, 75, and 80 wt %.

The behavior of magneto-polymer composites in the steady-state shear mode was analyzed by measuring the MRF flow curves in the absence of a magnetic

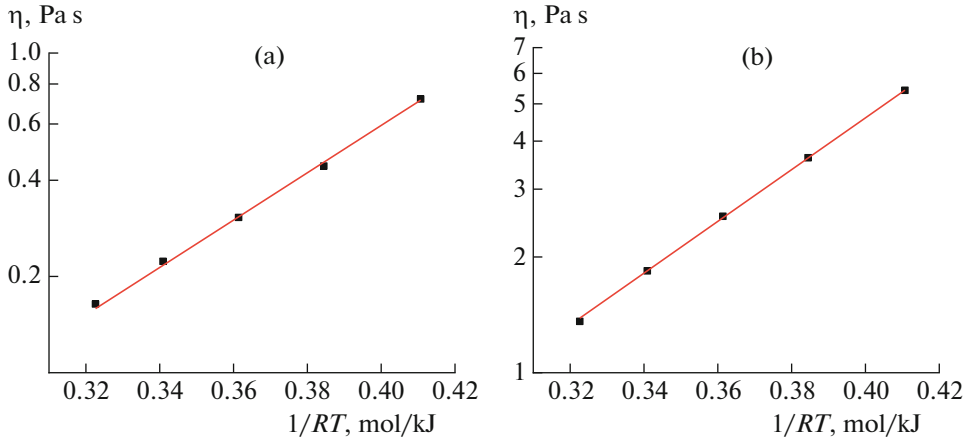

Fig. 3. Temperature dependences of viscosity in Arrhenius coordinates for (a) star-shaped and (b) linear PDMS.

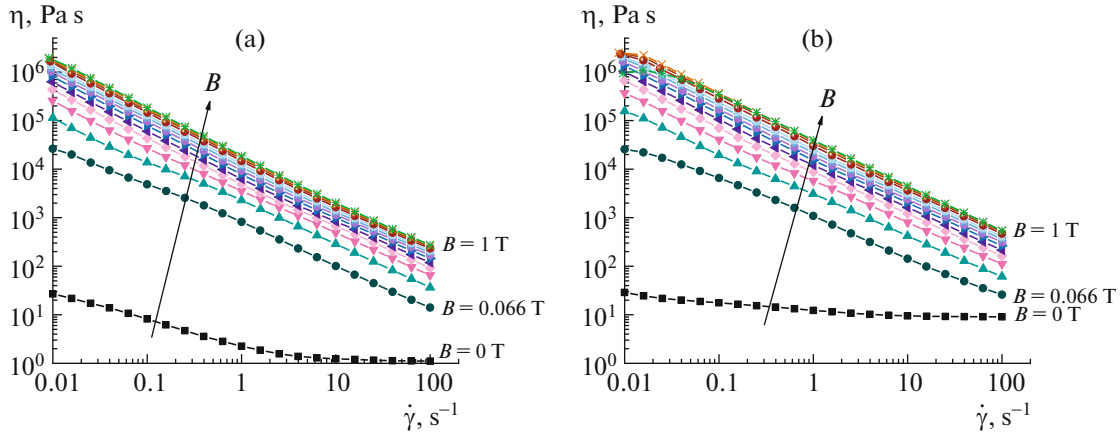

Fig. 4. Dependences of the viscosity of MRF-70 based on (a) star-shaped and (b) linear PDMS on the shear rate in various magnetic fields.

field and in magnetic fields of up to 1 T. Figure 4 shows the dependences of the viscosity of MRF-70 based on linear and star-shaped PDMS on the shear rate in various magnetic fields. MRFs with a magnetic filler mass content of 75 and 80% demonstrate qualitatively similar behavior (Supplementary Materials). Viscosities of all the obtained MRFs are presented in Table 1.

When the filler is added to the polymer liquid, its viscosity increases by several times in the absence of a magnetic field. For example, the viscosity of MRF-80 is approximately four times (Table 1) higher than the viscosity of a pure polymer liquid for the compositions based on both linear PDMS and star-shaped PDMS. In addition, in contrast to pure liquids with a Newtonian nature of flow, filled compositions exhibit a pronounced non-Newtonian behavior (Fig. 4). A drop in viscosity at high shear rates is characteristic of filled liquids [36] and is related to the fact that the filler particles are structured under application of the shear field and form concentric rings; as a result, the resistance to flow is reduced [37]. In [29], for magnetic compositions based on hyperbranched decyl polycarbosilanes with different magnetic filler content, a deviation from the Newtonian flow was observed when the content of magnetic particles was more than 72 wt %.

Under application of the magnetic field, the viscosity of the MRFs increases significantly and the dependence of the viscosity on the shear rate becomes even more significant. The increase in viscosity may be explained by the fact that magnetic interactions between filler particles are activated in the magnetic field. Owing to dipole-dipole magnetic interactions, the particles tend to arrange in chain structures along magnetic field lines. These chains are directed perpendicular to the shearing force, which hinders the flow. At high shear rates, the magnetic filler network breaks mechanically and its contribution to the total viscosity drops significantly.

Figure 5 shows the dependences of the viscosity of the MRFs with different content of magnetic particles on the magnitude of the external magnetic field. It can be seen that all MRFs demonstrate a colossal magnetic response. The graphs presented in logarithmic coordinates show that a significant increase in viscos-

Table 1. The viscosity of the obtained MRFs in the absence of the magnetic field and in the magnetic field $B = 1$ T at shear rate $\dot{\gamma} = 100\ s^{-1}$

Dispersion medium	Magnetic composition	η ($B = 0$ T), Pa s	η ($B = 1$ T), Pa s	$\frac{\eta(B = 1\,T)}{\eta(B = 0\,T)}$
Star-shaped PDMS	MRF-70	1.11	274	247
	MRF-75	2.14	343	160
	MRF-80	3.16	409	129
Linear PDMS	MRF-70	9.08	550	61
	MRF-75	11.5	691	60
	MRF-80	19	805	42

ity occurs even at low values of the magnetic field $B =$ 0.066 T, while in the maximum field $B = 1$ T, it is four orders of magnitude. An increase in the concentration of the magnetic filler in the investigated range leads only to a slight increase in the absolute value of the viscosity in the maximum magnetic field. Presumably, the most significant factor is overcoming the percolation threshold which can be reached even with a magnetic particle content of 70 wt %, as well as possible compositional heterogeneity.

The relative magnetic response of compositions based on the star-shaped PDMS is several times higher than the response of compositions based on the linear PDMS. This result is due to a lower initial viscosity of the medium. For this reason the particles of the magnetic filler experience much less resistance during restructuring. In this case, in the magnetic field, the contribution of the network of the magnetic filler turns out to be the most significant, so that the viscosity of the composite depends much more weakly on the initial viscosity of the dispersion medium.

An important feature of the rheological behavior of MRFs is the appearance of the yield stress under application of the magnetic field, which is not observed in the absence of the magnetic field. At rest, magnetic particles form a spatial network due to magnetic interactions. Magnetic forces restrict the movement of volume elements and give the composition the properties of a solid with an infinitely high viscosity. Only after the external mechanical force overcomes the magnetic forces the network of the magnetic filler breaks and the solid turns into a liquid. The yield stress τ_0 for the obtained MRFs was determined by fitting the flow curves measured at different magnitudes of the magnetic field using the Bingham equation [36]:

$$\tau = \tau_0 + k\dot{\gamma}, \quad \text{at} \quad \tau \geq \tau_0. \qquad (1)$$

The dependences of the yield stress of all the studied MRFs on the magnetic field strength are shown in Fig. 6. It is seen that the quantity τ_0 increases significantly with increasing field and concentration of magnetic particles. In the maximum magnetic field, the yield stress reaches 70 and 35 kPa for MRF-80 based on the linear PDMS and star-shaped PDMS, respectively. Such values of τ_0 are typical for MRFs [2, 24, 38]. It should be noted that, with the same content of magnetic particles, the use of star-shaped PDMS as a dispersion medium in MRFs reduces the value of τ_0, apparently, owing to a lower viscosity of the polymer. At the same time, the low viscosity of the composition based on the star-shaped PDMS and the absence of the zero-field yield stress can potentially allow the use of MRFs in braking mechanisms.

Viscosity of MRFs in the Transient Mode

The viscosities of the obtained magnetic compositions were measured in the cyclic switching on/switching off of the magnetic field under stationary shearing at a constant shear rate $\dot{\gamma} = 10\ s^{-1}$. During measurements, the magnetic field was switched on cyclically for 1 min and then switched off for 3 min. From the data presented in Fig. 7, one can conclude that, when the magnetic field is turned on, the viscosity of the magnetic composite reaches a stationary value rather quickly: the measurement accuracy is 3 s per point, and this time is sufficient to observe the viscosity reaching a plateau. When the magnetic field is turned off, the characteristic relaxation times of viscosity to a stationary value are several tens of seconds. It is also worth noting that there is a good repeatability of the properties of all MRFs in different cycles of switching on/switching off of the magnetic field starting from the second cycle. The first cycle differs from all subsequent ones because of a small residual magnetization of the metal protective casing with which the measuring setup is equipped.

Dynamic Mechanical Analysis of MRFs

Figure 8 presents the frequency dependences of the storage modulus of the MRFs measured in the absence of the magnetic field and in the maximum field $B = 1$ T. The values of the moduli measured at the frequency of shear vibrations oscillation frequency $\omega = 10$ rad/s and their relative change under application of the field are given in Table 2.

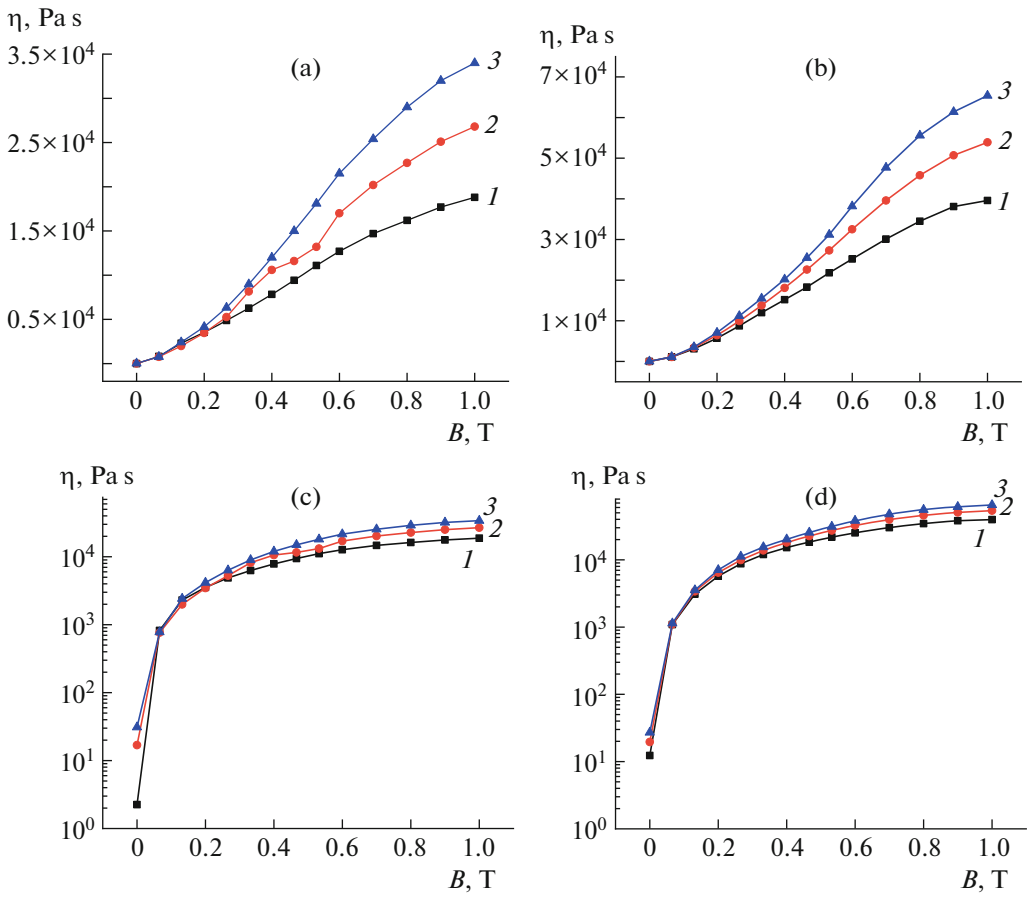

Fig. 5. Dependences of the viscosity of magnetic compositions (*1*) MRF-70, (*2*) MRF-75, and (*3*) MRF-80 based on (a, c) star-shaped and (b, d) linear PDMS on the magnitude of the magnetic field at the shear rate $\dot{\gamma} = 1\ s^{-1}$ on a (a, b) linear and (c, d) logarithmic scale along the *y* axis.

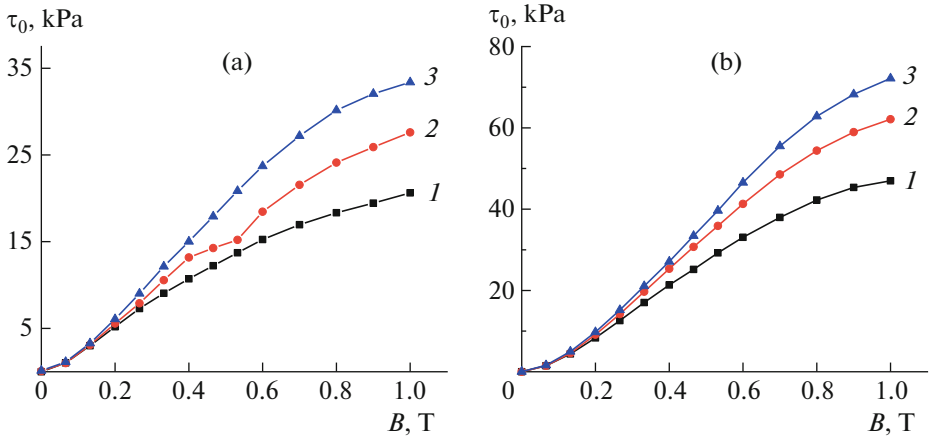

Fig. 6. Dependences of the yield stress of (*1*) MRF-70, (*2*) MRF-75, and (*3*) MRF-80 based on (a) star-shaped and (b) linear PDMS on the magnitude of the magnetic field.

In the absence of the magnetic field, both components of the complex dynamic modulus of the MRFs grow with an increase in the concentration of the magnetic filler. Their values are several times higher for the MRFs based on the linear PDMS owing to contribution of the polymer matrix. Under application of the magnetic field, the values of both G' and G'' increase considerably; the growth of G' reaches several orders

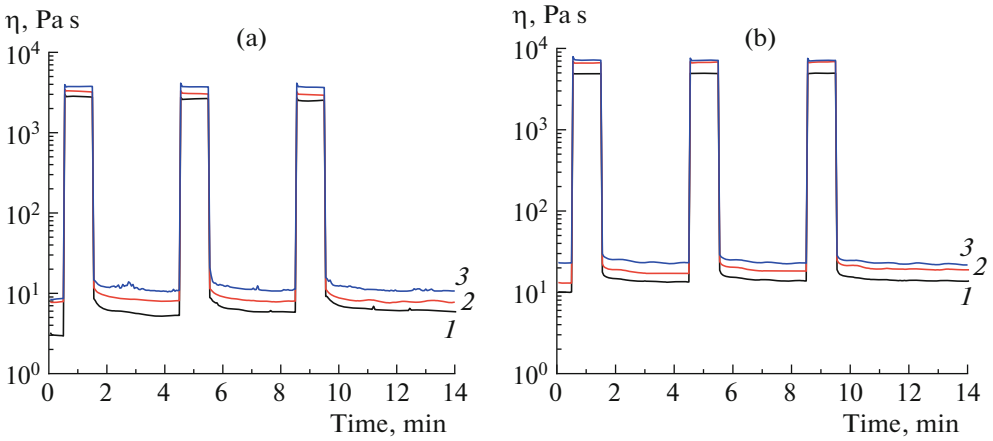

Fig. 7. Time dependence of the viscosity of (*1*) MRF-70, (*2*) MRF-75, and (*3*) MRF-80 with sequential switching on/switching off of the magnetic field for (a) star-shaped and (b) linear PDMS.

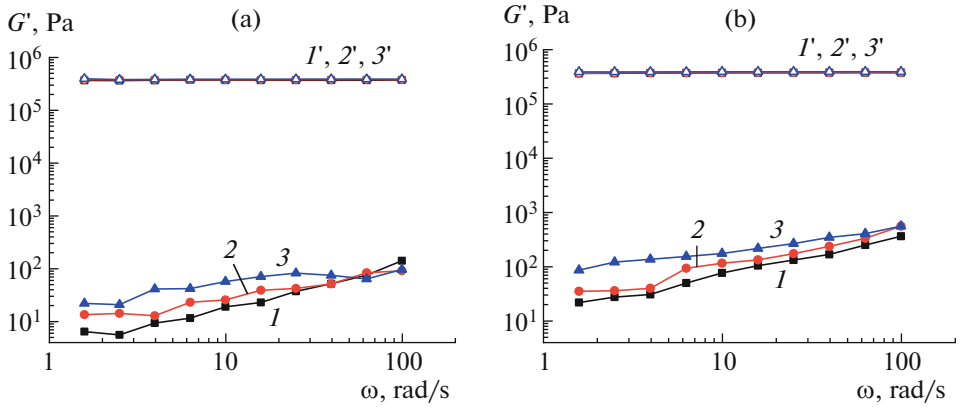

Fig. 8. Dependences of the storage modulus of (*1*, *1*') MRF-70, (*2*, *2*') MRF-75, and (*3*, *3*') MRF-80 based on (a) star-shaped and (b) linear PDMS on the angular frequency of shear oscillations (*1*–*3*) in the absence of a magnetic field and (*1*'–*3*') in the maximum magnetic field.

of magnitude. In the magnetic field, the values of the storage modulus for MRFs based on the star-shaped and linear PDMS are approximately the same; they slightly increase with an increase in the filler concentration. Apparently, this behavior of the material is associated with the fact that in the magnetic field the elastic response is mainly determined by the contribution of the network formed by the magnetic filler, which turns out to be significant owing to strong magnetic interactions of iron microparticles. Against this

Table 2. Rheological characteristics of MRFs at an angular frequency of shear oscillations ω = 10 rad/s and oscillation amplitude $\gamma_0 = 0.2\%$

Dispersion medium	Magnetic composition	G' ($B = 0$ T), Pa	G'' ($B = 0$ T), Pa	$\frac{G'(B = 1\,\text{T})}{G'(B = 0\,\text{T})}$	$\frac{G''(B = 1\,\text{T})}{G''(B = 0\,\text{T})}$
Star-shaped PDMS	MRF-70	15.8	32.4	24000	118
	MRF-75	26.4	49.6	15000	62.5
	MRF-80	51.8	83.5	8000	34.1
Linear PDMS	MRF-70	43.6	128	8200	80
	MRF-75	50.5	230	7700	18.1
	MRF-80	88.2	331	4700	7.5

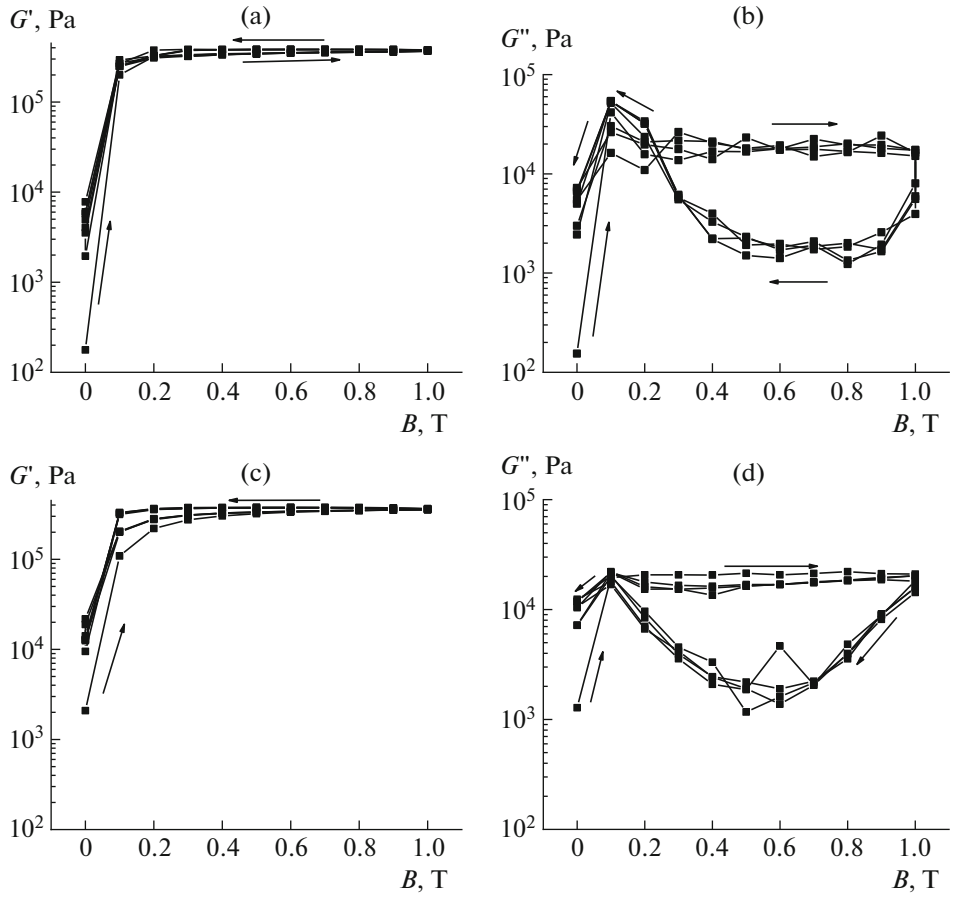

Fig. 9. Dependences of (a, c) the storage modulus and (b, d) the loss modulus of MRF-70 based on (a, b) star-shaped and (c, d) linear PDMS on the magnitude of the magnetic field with its cyclic increase/decrease.

background, the elastic contribution of the dispersion medium is small. In addition, since the elastic modulus in the absence of the magnetic field substantially depends on the type of polymer matrix, the relative growth of the dynamic shear modulus components for magnetic composites based on the star-shaped PDMS is several times higher than that for compositions based on the linear PDMS. As noted above, a similar behavior was described for the static viscosity of the compositions.

It should be noted that the loss modulus in the magnetic field decreases with an increase in the concentration of the magnetic filler, in contrast to the behavior in the absence of the field (Table 2). The magnetic field induces strong magnetic interactions between the particles which grow with an increase in the degree of filling of the composite, preventing the destruction of aggregates of magnetic particles under application of the external mechanical load.

The dependences of G' and G'' on the magnitude of the external magnetic field were plotted, and the hysteresis of the rheological characteristics of the MRFs in the magnetic field was studied. Four cycles of measurements of the components of the complex dynamic modulus were carried out with an increase in the magnetic field to a maximum value of 1 T and its subsequent decrease to zero. The corresponding dependences for MRF-70 based on the star-shaped and linear PDMS are shown in Fig. 9; for compositions MRF-75 and MRF-80, these dependences are available in Supplementary Materials.

With an increase in the magnetic field, the main changes in the storage modulus in the first cycle and subsequent ones occur in fields from 0 to 100–200 mT when, apparently, the main restructuring of the filler structure takes place. When $B > 200$ mT, the storage modulus continues to grow slightly, but the change in its value is insignificant. On the contrary, the loss modulus after reaching a maximum at $B = 100$ mT slightly decreases with a further increase in the field. This can be explained by strengthening of the filler structure due to the enhancement of magnetic interactions.

In the oscillatory oscillation mode, after each cycle of increasing/decreasing the magnitude of the applied field, a significant increase in the components of the complex shear modulus occurs when the field is removed. A significant hysteresis of the loss modulus

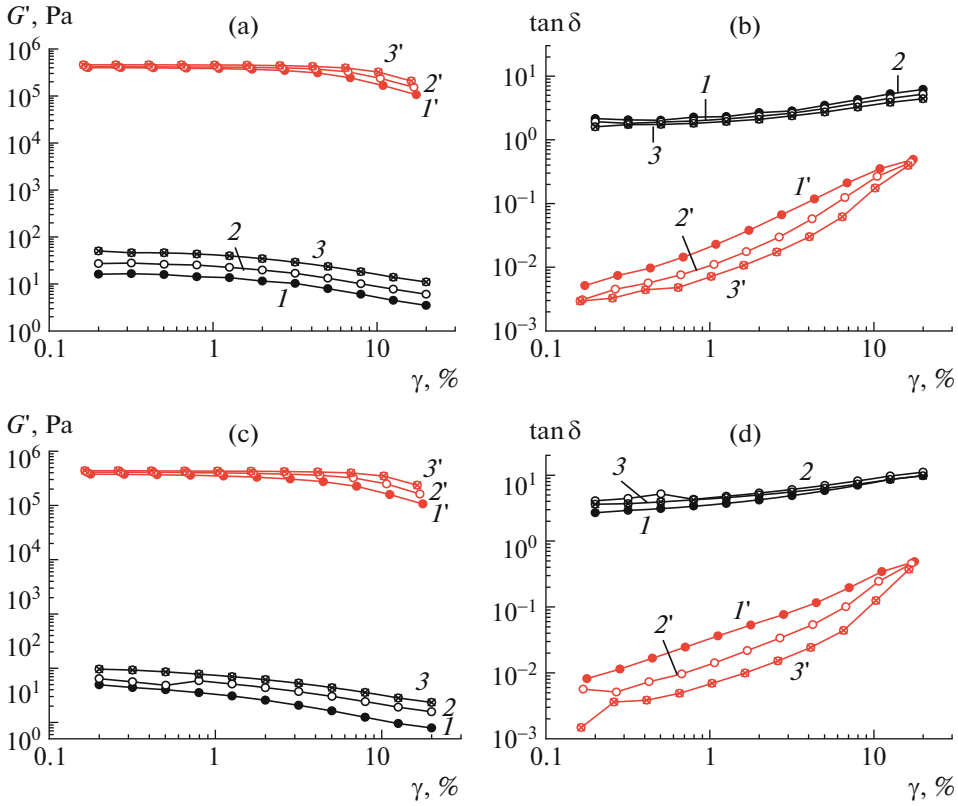

Fig. 10. Dependences of (a, c) the storage modulus and (b, d) the loss modulus of (*1*, *1'*) MRF-70, (*2*, *2'*) MRF-75, and (*3*, *3'*) MRF-80 based on (a, b) star-shaped and (c, d) linear PDMS on the amplitude of shear oscillation strain shear strain amplitude in the absence of the magnetic field and in the maximum magnetic field $B = 1$ T.

is also observed when increasing and decreasing the magnetic field. It was previously noted that magneto-mechanical hysteresis is a property inherent in magneto-polymer composites based on both crosslinked polymer matrices [39–42] and liquid dispersion media [29]. It is associated with the processes of rearrangement of the structure formed by microparticles of the magnetic filler which are determined not only by the magnitude of the magnetic field but also by the prehistory of evolution under simultaneous application of the field and mechanical load. Owing to the magnetic adhesion of particles in aggregates formed with an increase in the magnetic field, the elastic response of the material remains high even with a decrease in the field to values of about 400 mT and the energy dissipation is minimal. Only when the magnetic field decreases below the critical value particle aggregates begin to break down by the external mechanical force, which leads to an increase in energy dissipation and a decrease in the storage modulus of the material.

It is known that filled elastomers exhibit the Payne effect [43, 44]. This phenomenon consists in the fact that, with an increase in the strain amplitude, the storage modulus of the material decreases and the loss modulus passes through a maximum with the maximum occurring in the region of the sharpest drop in the storage modulus. This is due to the fact that large deformations destroy the aggregates formed by the filler particles. It was recently noted [45, 46] that, in the case of using ferromagnetic microparticles as a filler, the Payne effect becomes more pronounced owing to strong magnetic interactions in the aggregates of magnetic particles that are formed under application of the magnetic field. These aggregates are stable under weak mechanical loads but are destroyed under high shear deformations. The term "magnetic Payne effect" was even introduced in [47]. It is clear that such an effect should also be inherent in magnetorheological fluids exhibiting viscoelastic behavior in a magnetic field which is close to the behavior of solids. Indeed, the magnetic Payne effect in magnetorheological fluids was observed and studied in detail in recent works [29, 48].

Typical dependences $G'(\gamma)$ for the MRFs studied in this work are shown in Figs. 10a and 10c. The storage modulus decreases several times with a change in the strain amplitude γ from 0.2 to 20%. In this case, in the magnetic field $B = 1$ T, the region of linear viscoelasticity expands, which is associated with the strengthening of the magnetic filler network in the magnetic field. The higher the concentration of magnetic parti-

cles in the MRFs, the higher the shear strains at which a noticeable softening of the composite begins, which is also related to the enhancement of magnetic interactions.

Figures 10b and 10d show the dependences of the mechanical loss tangent (the loss factor) $\tan\delta = G''/G'$ on the strain amplitude. The loss factor characterizes the ratio of the contribution of the viscous response of the sample to the elastic one. If $\tan\delta > 1$, then the viscous response prevails; if $\tan\delta < 1$, the elastic response dominates. It can be seen that, in the entire investigated region of strain amplitudes in the absence of the magnetic field, all MRFs behave like liquids. In this case, when the magnetic field is switched on, the main contribution to the viscoelastic properties is already made by a strong network of the magnetic filler, owing to which $\tan\delta < 1$; i.e., the elastic contribution to the material properties dominates. It should be noted that, in the region of small strain amplitudes, the drop in $\tan\delta$ upon application of the magnetic field $B = 1$ T reaches almost three orders of magnitude, which indicates the possibility of regulating the damping properties of the obtained MRFs in a wide range.

CONCLUSIONS

In this work, the magnetorheological fluids were obtained using new polymer dispersion media (linear and star-shaped PDMS) and carbonyl iron magnetic microparticles with a mass content of 70, 75, and 80 wt %. A comparative analysis of their rheological behavior demonstrated that all the obtained compositions have a high magnetorheological effect: the increase in the viscosity and storage modulus reaches four orders of magnitude in a magnetic field up to 1 T.

The main effect of the dispersion medium is manifested in the properties of the MRFs in the absence of the magnetic field: owing to a more compact structure of star-shaped PDMS macromolecules, the magnetorheological fluids based on it have a significantly lower viscosity than their analogs based on the linear PDMS, despite the lower molecular weight of the latter. The dependence of the viscosity of the MRFs on the viscosity of the dispersion medium in the magnetic field is much weaker: at low shear rates, the main contribution is made by the aggregation of magnetic particles; this contribution grows with an increase in the concentration of the magnetic filler. In the magnetic field, the viscosity values of 0.19–0.65 MPa s are achieved at a shear rate of 1 s^{-1}. The relative magnetic response of the MRFs based on the star-shaped PDMS is higher than that of the MRFs based on the linear PDMS owing to the lower initial viscosity of the medium. The formation of a strong magnetic filler network in the magnetic field causes appearance of the yield stress, which in the MRFs based on the linear and star-shaped PDMS at $B = 1$ T reach high values of 70 and 35 kPa, respectively.

The aggregation of magnetic particles under application of the magnetic field also makes a decisive contribution to the dynamic mechanical response of magneto-polymer compositions. It is shown that, in the region of linear viscoelasticity, the shear storage modulus of the MRFs reaches several hundred kilopascals. The maximum relative increase in the components of the complex dynamic modulus is observed for the MRFs based on the star-shaped PDMS with a mass concentration of carbonyl iron of 70 wt %. One should note a significant, up to three orders of magnitude, drop in the mechanical loss tangent, which indicates that the damping properties of the obtained MRFs can be regulated in a wide range.

ACKNOWLEDGMENTS

The NMR investigations and GPC analysis were performed in the Collective Usage Center of the Institute of Synthetic Polymer Materials, Russian Academy of Sciences. Access to electronic scientific resources was provided by Moscow State University and A.N. Nesmeyanov Institute of Organoelement Compounds of Russian Academy of Sciences with support of the RF Ministry of Education and Science.

FUNDING

S.A. Kostrov is grateful to the Theoretical Physics and Mathematics Advancement Foundation BASIS for financial support.

The study was supported by the Russian Science Foundation (project no. 19-13-00340).

SUPPLEMENTARY INFORMATION

The online version contains supplementary material available at https://doi.org/10.1134/S0965545X2103007X

REFERENCES

1. J. De Vicente, D. J. Klingenberg, and R. Hidalgo-Alvarez, Soft Matter **7**, 3701 (2011).
2. J. D. Carlson and M. R. Jolly, Mechatronics **10**, 555 (2000).
3. S. K. Mangal and V. Sharma, J. Braz. Soc. Mech. Sci. Eng. **39**, 4191 (2017).
4. M. S. A. Rahim, I. Ismail, S. A. Wahid, S. Aid, and S. N. Aqida, MATEC Web Conf. **90**, 01061 (2017).
5. S. E. Premalatha, R. Chokkalingam, and M. Mahendran, Am. J. Polym. Sci. **2** (4), 50 (2012).
6. S. Genç and P. P. Phulé, Smart Mater. Struct. **11**, 140 (2002).
7. X. Zhu, X. Jing, and L. Cheng, J. Intell. Mater. Syst. Struct. **23**, 839 (2012).
8. X. Yuan, T. Tian, H. Ling, T. Qiu, and H. He, Shock Vib. **2019**, article ID 1498962 (2019).
9. D. Cruze, G. Hemalatha, S. V. S. Jebadurai, L. Sarala, D. Tensing, and S. J. E. Christy, Civil Eng. J. **4**, 3058 (2018).
10. A. Muhammad, X. Yao, and Z. Deng, J. Marine Sci. Appl. **5** (3), 17 (2006).
11. J. Li, W. Wang, Y. Xia, H. He, and W. Zhu, Appl. Phys. Lett. **106**, 014104 (2015).
12. X. X. Bai, S. Shen, F. L. Cai, X. C. Deng, and S. X. Xu, in *Active and Passive Smart Structures and Integrated Systems XII,* Ed. by A. Erturk (SPIE - International Society for Optics and Photonics, Denver, 2018), Vol. 10595, p. 1059507.
13. H. Deng, M. Wang, G. Han, J. Zhang, M. Ma, X. Zhong, and L. Yu, Smart Mater. Struct. **26**, 125014 (2017).
14. C. Sarkar and H. Hirani, Proc. Inst. Mech. Eng., Part D **229**, 1907 (2015).
15. J. Wu, H. Li, X. Jiang, and J. Yao, Smart Mater. Struct. **27**, 025016 (2018).
16. T. Le-Duc, V. Ho-Huu, and H. Nguyen-Quoc, Smart Mater. Struct. **27**, 075060 (2018).
17. US Patent No. 9016373 (2015).
18. US Patent No. 15308675 (2017).
19. US Patent No. 16389154 (2019).
20. D. W. Felt, M. Hagenbuchle, J. Liu, and J. Richard, J. Intell. Mater. Syst. Struct. **7**, 589 (1996).
21. A. H. Dorosti, M. Ghatee, and M. Norouzi, J. Magn. Magn. Mater. **498**, 166193 (2020).
22. P. Ranjan, R. Balasubramaniam, and V. K. Jain, J. Micromanuf. **1** (1), 45 (2018).
23. F. Jonsdottir, K. H. Gudmundsson, T. B. Dijkman, F. Thorsteinsson, and O. Gutfleisch, J. Intell. Mater. Syst. Struct. **21**, 1051 (2010).
24. S. K. Mangal and V. Sharma, J. Braz. Soc. Mech. Sci. Eng. **39**, 4191 (2017).
25. L. Fan, G. Wang, W. Wang, H. Lu, F. Yang, and X. Rui, J. Mater. Sci. **54**, 1326 (2019).
26. Y. P. Seo, S. Han, J. Choi, A. Takahara, H. J. Choi, and Y. Seo, Adv. Mater. **30**, 1704769 (2018).
27. J. Sutrisno, A. Fuchs, H. Sahin, and F. Gordaninejad, J. Appl. Polym. Sci. **128**, 470 (2013).
28. V. V. Gorodov, S. A. Kostrov, R. A. Kamyshinskii, E. Y. Kramarenko, and A. M. Muzafarov, Russ. Chem. Bull. **67**, 1639 (2018).
29. V. G. Vasiliev, N. A. Sheremetyeva, M. I. Buzin, D. V. Turenko, V. S. Papkov, I. A. Klepikov, and E. Y. Kramarenko, Smart Mater. Struct. **25**, 055016 (2016).
30. N. G. Vasilenko, E. A. Rebrov, A. M. Muzafarov, B. Eßwein, B. Striegel, and M. Moller, Macromol. Chem. Phys. **199**, 889 (1998).
31. O. V. Novozhilov, I. V. Pavlichenko, N. V. Demchenko, A. I. Buzin, N. G. Vasilenko, and A. M. Muzafarov, Russ. Chem. Bull. **59**, 1909 (2010).
32. M. Cvek, M. Mrlik, R. Moucka, and M. Sedlacik, Colloids Surf., A **543**, 83 (2018).
33. P. A. Tikhonov, N. G. Vasilenko, G. V. Cherkaev, V. G. Vasiliev, N. V. Demchenko, E. A. Tatarinova, and A. M. Muzafarov, Mendeleev Commun. **29**, 625 (2019).
34. E. A. Sidorovich, Polym. Sci., Ser. A **37**, 2020 (1995).
35. M. V. Sobolevskii, I. I. Skorokhodov, and K. P. Grinevich, *Oligoorganosiloxanes. Properties, Production, Application* (Khimiya, Moscow, 1985) [in Russian].
36. A. Ya. Malkin, Rheology Principles (Tsentr Obrazovatel'nykh Programm Professiya, St. Petersburg, 2018) [in Russian].
37. G. Shramm, *Practical Rheology and Rheometry Foundations* (Koloss, Moscow, 2003) [in Russian].
38. X. Tang, X. Zhang, R. Tao, and Y. Rong, J. Appl. Phys. **87**, 2634 (2000).
39. V. V. Sorokin, G. V. Stepanov, M. Shamonin, G. J. Monkman, A. R. Khokhlov, and E. Yu. Kramarenko, Polymer **76**, 191 (2015).
40. I. A. Belyaeva, E. Y. Kramarenko, and M. Shamonin, Polymer **127**, 119 (2017).
41. I. A. Belyaeva, E. Y. Kramarenko, G. V. Stepanov, V. V. Sorokin, D. Stadler, and M. Shamonin, Soft Matter **12**, 2901 (2016).
42. M. Shamonin and E. Y. Kramarenko, *Novel Magnetic Nanostructures* (Elsevier, Amsterdam, 2018).
43. A. R. Payne, Appl. Polym. Sci. **6** (19), 57 (1962).
44. S. Richter, M. Saphiannikova, K. W. Stöckelhuber, and G. Heinrich, Macromol. Symp. **291**, 193 (2010).
45. H. An, S. J. Picken, and E. Mendes, Polymer **53**, 4164 (2012).
46. Y. Tong, X. Dong, and M. Qi, Comp. Commun. **15**, 120 (2019).
47. H. N. An, B. Sun, S. J. Picken, and E. Mendes, J. Phys. Chem. B **116**, 4702 (2012).
48. I. Arief and P. K. Mukhopadhyay, J. Alloys Compd. **696**, 1053 (2017).